

# Characterization of the electromagnetic shielding and compressive behavior of a highly porous titanium foam with spherical pores

P.S. Liu<sup>a)</sup> and G. Cui

Key Laboratory of Beam Technology and Material Modification of Ministry of Education, College of Nuclear Science and Technology, Beijing Normal University, Beijing 100875, China

(Received 16 July 2015; accepted 22 September 2015)

A novel sort of cellular titanium foam with the porosity of 86–90% and the main-pore size of 0.5–3.0 mm was successfully prepared. Such foam exhibited a compressive curve showing three regimes: the initial elasticity, the middle zigzag plateau, and the final “densification.” This “densification” presented a course that the broken pieces continually accumulated in those pores which were unbroken or not entirely broken. The fracture morphology suggested that the compressive failure was typically brittle for this titanium foam. The electromagnetic shielding performance was investigated in the radio wave frequency range (0.3–3000 MHz) for this foam, which showed an evident effectiveness with a good performance at low frequencies. On the whole, the effectiveness would be superior while the porosity of the sample was relatively small. It could be inferred that the present foam samples would perform their electromagnetic shielding mainly by the reflection loss mechanism in the low-frequency range, and give priority to the absorption loss mechanism at the upper-frequencies.

## I. INTRODUCTION

Metal foams are porous materials with dual attribute of structural and functional actions, and may be used as the lightweight structure that can reduce noises, absorb energies, attenuate shock, shield electromagnetic waves, or resist the fire in a number of fields such as the aerospace, automobile, communication, ship, and construction industries.<sup>1–5</sup> There have been lots of researches on aluminum foams, but relatively a little on other metal foams, such as the titanium foam. Owing to the high melting point and the excellent corrosion resistance of metallic titanium or its alloy, titanium foams could be more suitable than aluminum foams for the more rigorous demand on the ambient temperature and the service environment.

Unlike aluminum foams that have been widely used and easy to produce, cellular titanium foams with high porosity are difficult to obtain,<sup>6–9</sup> due to the high melting temperature and easy oxidation of titanium. Not only the preparation technology for titanium foams need be different from that for aluminum foams, but also the resultant porous products would have their own individual behaviors in their properties.

Titanium foams are attractive for structural and biomedical applications,<sup>6,10</sup> and they have been already studied largely on implant materials,<sup>9–13</sup> but seldom on engineering

materials. Porous implant materials require their pores to be three-dimensionally interconnected fully to facilitate the transport of body fluids, indicating a reticular open-cell structure.<sup>14,15</sup> By comparison with this porous structure, the cellular titanium foam has been quite rarely researched.<sup>13</sup> As well known, metal foams will be developed for lower bulk density and higher porosity when the structural weight becomes important. As for porous metal foams based on different practical applications, the basic mechanical property is always the most elementary.<sup>1,16–19</sup> Accordingly, a high porosity titanium foam with cellular structure was firstly prepared in the present work, and its compressive behavior, one of the most elementary mechanical properties, was preliminarily investigated.

Electromagnetic radiation may bring a poor performance of electronic instruments and equipments, and possibly lead to the information leakage.<sup>20–22</sup> With a broader and broader application of electronic products, electromagnetic pollution has had a more and more far-reaching involvement in the environmental and military security, and the quest for safeguards against electromagnetic radiation with radio efficiency has thus become a burgeoning area of research.<sup>23</sup> In modern world full of electronic products, one of the most important issues is a need to shield the electric devices from electromagnetic interferences (EMI).<sup>20</sup> Therefore, the researches on EMI shielding are getting more and more attention,<sup>22</sup> and a critical requirement for EMI-shielding material is of low weight, so conductive porous materials are good candidates.<sup>23</sup> Nevertheless, there were only a few relevant researches on metal foams.<sup>21–25</sup> As a practical performance with the promising prospect of applications for

Contributing Editor: Paolo Colombo

<sup>a)</sup>Address all correspondence to this author.

e-mail: Liu996@263.net

DOI: 10.1557/jmr.2015.308

metal foams, the electromagnetic shielding effectiveness was also preliminarily investigated for the present titanium foam in this paper.

## II. PREPARATION OF THE TITANIUM FOAM

Using the space-holder method combined with the molten powder foaming process,<sup>2,5</sup> a sort of cellular titanium foam with high porosity was prepared with titanium (Ti) powder as the main raw material and nickel (Ni) as the main alloy element. The pure titanium powder and the pure nickel powder with both the size of  $-300$  meshes were firstly selected by the mass ratio of 75:25–85:15 to uniformly mix together for 2 h, and then in the resultant mixed metallic powder a certain amount of the self-made spherical foamer (e.g., the spherical particle made from the mashed cocoon or the flour, constituting 80–85% of the mixture by volume, and the experimental result showed the latter not to be good in this work), the nontoxic adhesive (e.g., the jellylike matter from modulating the potato starch and solvent) and the appropriate amount of the required additive (such as ammonium bicarbonate powder) were added according to the set porosity of the product. Evenly blended, the prefabricated product was afterward made by pressing in a mold to dry. The prefabricated product after drying was placed in a nonoxidizing environment together with the mold, and rapidly heated to 1000–1200 °C to sinter and then cooled, during which the organic species carried out a thermal decomposition to remove the space holder, resulting in a highly porous product of titanium foam. In the process of sintering at 1000–1200 °C, some powder-like  $\text{Ti}_2\text{Ni}$  alloy (see Fig. 1) could form and melt in the green body, which would be very helpful to combining metallic powders into one whole. The resultant porous product with porosity of about 90% is shown in Fig. 2 as an example. Figure 2(a) shows the sample with the main

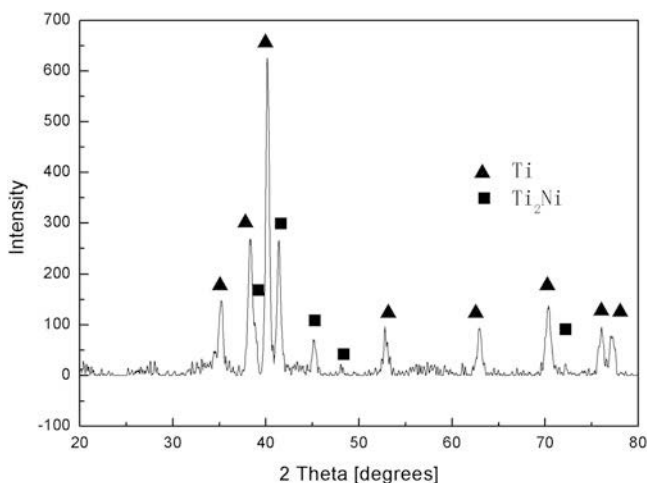


FIG. 1. X-ray diffraction result of the titanium foam product.

pores of millimeter-scaled spherical shape. Such product is of high porosity, so the main pores cannot be closed generally and are connected with each other by the small holes [Fig. 2(b)]; the example of the macroscopically “dense” wall structure [Fig. 2(c)] shows a good binding of the solid phase, and the irregular fine pores with micrometer size further increase the connectivity between the internal pores. The analytical result of x-ray diffraction (Fig. 1) revealed this product to be composed of the main phase of Ti and the second of  $\text{NiTi}_2$ , which is in agreement with that from the phase diagram of Ti–Ni alloys.

## III. COMPRESSIVE BEHAVIOR

### A. Experimental method

Owing to the structural feature, metal foams would deform in a very different way from traditional materials, so the test method of compression for traditional metal materials could not be fully applicable to porous metals. Therefore, the present titanium foam was performed a quasistatic compression test under a condition at room temperature by the following procedure, referring to the test method introduce in Ref. 1.

To obtain the sample suitable for compression test at the current processing level, a specially designed mold was used to make the columnar sample of titanium foam (see Fig. 2), which would be capable of executing the compression test. This sample was about 45 mm in

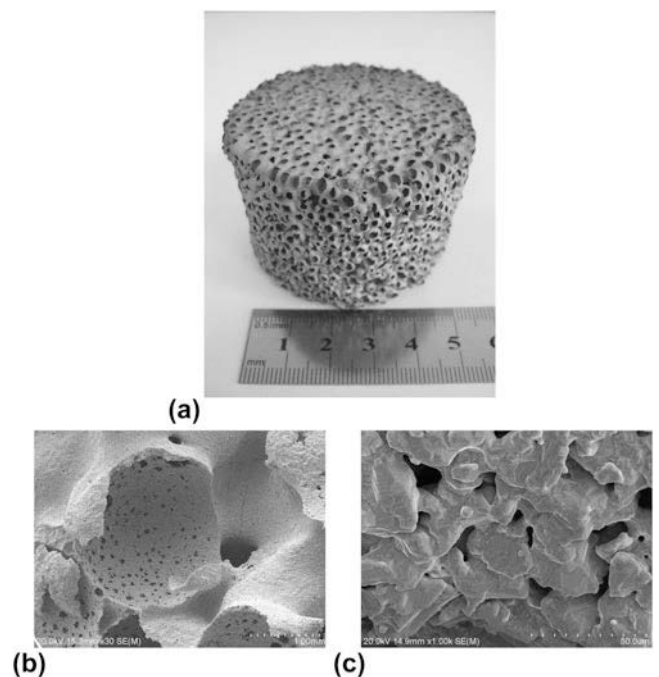


FIG. 2. Morphologies of the cellular titanium foam with spherical pores: (a) a cylindrical sample with high porosity; (b) a locally magnified image of the spherical pore structure; (c) the microporous structure of the cell wall.

diameter, 50 mm in height, and 86–90% in porosity. In the process of testing, two ends of the compression sample and the end of two pressure heads of the test equipment were all smeared with the graphite to make them smoother, so as to reduce the friction caused by the relative displacement of the sample end and the pressure head of the equipment, as much as possible. An electronic universal testing device (WDW-3050 type; Beijing United Test Co., Ltd., Beijing, China) controlled by microcomputer was for the compression test, with the maximum equipment load of 5 T and the compression velocity of 1 mm/min.

## B. Results and analysis

To know the relatively complete information about the compressive behavior of this cellular titanium foam with high porosity, the sample of about 90% porosity was selected to investigate the destroyed morphologies when compressed to the nominal strain of about 1/3 and 2/3, respectively, as well as the relationship between nominal stress and nominal strain during this compression. The morphology of the sample compressed to the nominal strain of about 1/3 (Fig. 3) suggests that the compressive failure of this titanium foam occurred to be continually pushed forward by the pore collapse and fracture in the way of layer by layer in the direction perpendicular to loading. Because the loading action by the equipment could result in a stress gradient in the sample, the pore layer close to the pressure head would be preferentially damaged. The broken pieces close to the brim of the joint surface between the sample and the pressure head would go outside off the sample, and those close to the interior of the joint surface would drop down inside the pores in the layer just beneath to make the sample gradually tend to “densification.” This failure mode that the pores collapsed in the way of layer by layer in the sample created a fluctuant plateau area with saw-tooth shape in the nominal stress–strain curve for the compressive

process (see Fig. 4). Since the pores did not very uniformly distribute within the actual sample, those located at other weak positions, although not close to the joint layer touching the pressure head, would also be preferentially ruined to promote the “densification” of the sample. Hence the zigzag plateau area in the nominal stress–strain curve showed a slowly upward tendency.

The morphology of the sample compressed to the nominal strain of about 2/3 (Fig. 5) displayed a thorough destruction of the titanium foam. The nominal stress–strain curve formed during this compression is shown in Fig. 6, which is relatively complete to present three regimes of the initial elasticity, the compressive plateau, and the densification. By comparison, only the first two regimes, i.e. the initial elasticity and the compressive plateau, appear in Fig. 4, not yet reaching the densification region due to the nominal strain just stopped at 1/3.

The initial elasticity region and the following zigzag plateau in the compressive curves in Figs. 4 and 6 indicate

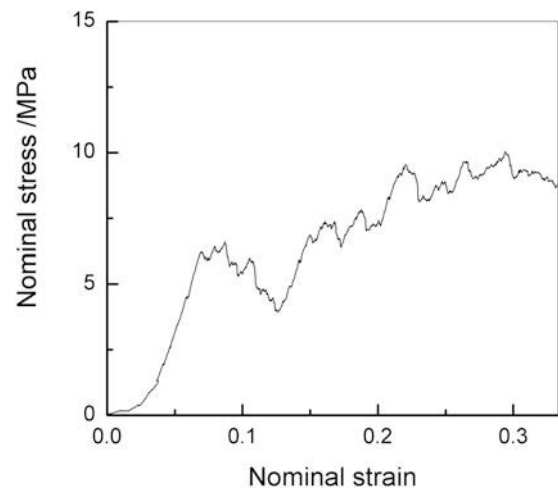


FIG. 4. Compressive curve with the nominal strain ended at about 1/3 for the sample of about 90% porosity.

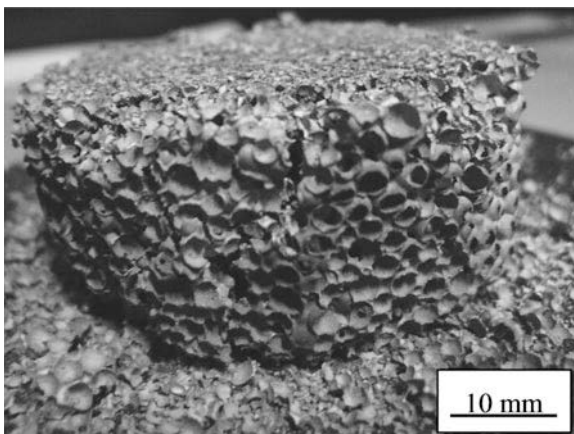


FIG. 3. Morphology of the about 90% porosity sample fractured at the nominal strain of about 1/3.

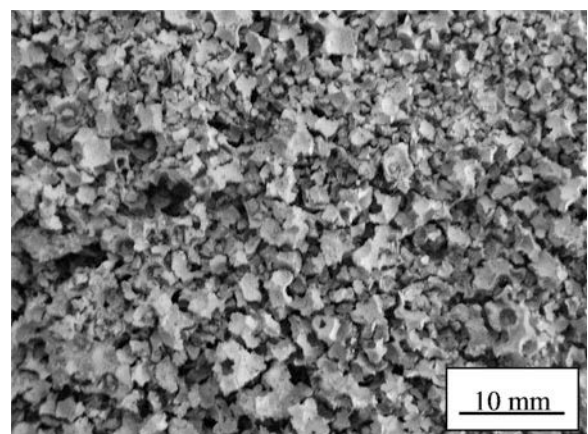


FIG. 5. Morphology of the about 89% porosity sample fractured at the nominal strain of about 2/3.

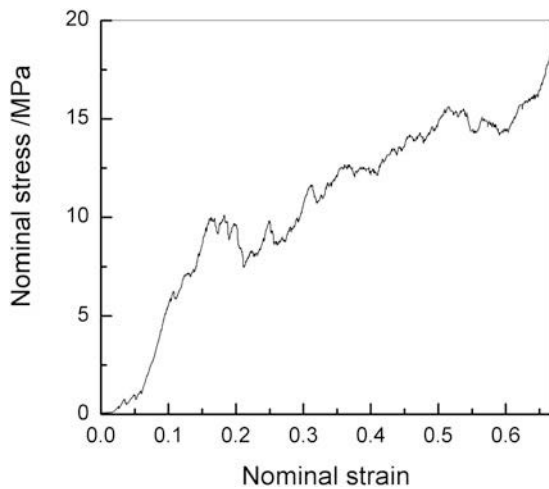


FIG. 6. Compressive curve with the nominal strain ended at about 2/3 for the sample of about 90% porosity.

that the present titanium foam would belong to a typical elastic–brittle porous material. This porous titanium alloy had its elastic deformation by cell wall bending when it was at low stress. With the gradual increase of stress, the porous structure began a brittle collapse when the stress was larger than the elastic limit of the cell wall, and the stress steeply decreased. After the first layer of pores collapsed and felled off, the second layer also worked as this, so a fluctuant zigzag plateau would show in the compressive curve. Continually collapsed pieces accumulated inside the pores that had not collapsed or not completely collapsed, resulting in the “densification” of the sample to finally cause the subsequent continual increase of the stress value. As we know, elastic–plastic foams have their compressive curve commonly showing three regimes of the initial elastic deformation, the yielding plateau in succession, and the final densification, for example, the aluminum foam, which is well known. The prominent differences between this kind of curves and the present compressive curve are as follows: the plateau is relatively smooth for the former, but markedly fluctuates for the latter; more noticeably, the compression should be equivalent to that of the corresponding dense material after densification for the former, to some extent, but for the latter there would be just a nominal densification that is of the increased accumulation of the broken pieces, and the resultant structure would deviate greatly from that of the corresponding dense material.

The limiting stress,  $\varepsilon_D$ , which is achieved at the beginning of “densification” during the compression, is described for foamed materials in Ref. 26:

$$\varepsilon_D = 1 - 1.4(1 - \theta) \quad , \quad (1)$$

where  $\theta$  is the porosity of the porous body. In Eq. (1) taking  $\theta = 89\%$ , a value of the porosity of the titanium

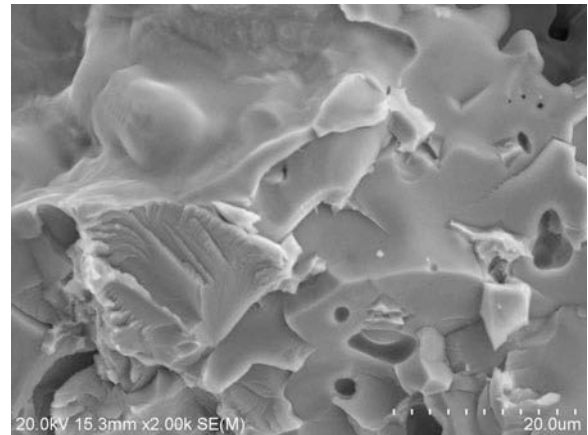


FIG. 7. SEM fracture image of the sample that was compressed to break: the pore-wall morphology at the fracture position.

foam sample corresponding to that in Fig. 6, gives the corresponding “densification” stress to be about 0.85. Figure 6 shows this limiting stress could actually reach only about 0.65, which is obviously less than 0.85. This is caused by the bridging support due to that the above-mentioned broken pieces resulted from the collapsed pores filled in those pores that were unbroken or not entirely broken, so the “densification” regime would arrive ahead of schedule on the compressive curve. The continual accumulation of the broken pieces inside the sample could make it incessantly tend to be “densified,” and finally the nominal stress would lead to a rapid increase with the increase of the nominal strain. On the present compressive curve, this final “densification” regime would come forth apparently earlier than that of those elastoplastic foamed materials. However, this “densification” had been resulted from the accumulation of the broken pieces in the pores, and there would be a lot of rigid gaps in the “densified” locality, which is quite different from the densified structure formed in the corresponding stage in the elastoplastic foamed materials.

To understand the microscopic morphology of the compressively damaged sample, a scanning electron microscopy of SEM4800 type made by Hitachi Company in Tokyo, Japan was also used to observe the fracture surface structure, with the resolution of 2.0 nm. As shown in Fig. 7, the fracture morphology of the pore-wall exhibits a clear cleavage surface, illustrating a brittle fracture which is corresponding to the zigzag plateau in the compressive curves in Figs. 4 and 6.

## IV. ELECTROMAGNETIC SHIELDING

### A. Experimental methods

The DR-S01 shielding effectiveness tester (Beijing Ding-rong Shichuang Science & Technology Co. Ltd., Beijing, China) was used to test the electromagnetic shielding

effectiveness for the present titanium foam samples. Such a complete set of equipment is shown in Fig. 8. This device is designed in accordance with the international standard of ASTM 4935-2010 “Standard test method of electromagnetic shielding effectiveness of planar materials”, and suitable for testing the plane wave shielding effectiveness of planar electromagnetic shielding materials, with a wide range of the effective testing frequency because of highly precise machining the coaxial flange parts. The emission frequency of 0.3–3000 MHz in this test covers the spectrum of radio waves.

The circular plate sample with the diameter of about 100 mm was made for the titanium foam to be used in the experiment of the electromagnetic shielding effectiveness. The pore parameters of the samples are listed in Table I.

### B. Results and analysis

The Schelkunoff theory indicates that the shielding effectiveness (SE, dB) of the shielding material includes the absorption loss ( $A$ ), the reflection loss ( $R$ ), and the multiple reflection loss ( $B$ )<sup>21,27,28</sup>:

$$SE = A + R + B \quad , \quad (2)$$

here:

$$A = at(f\mu_r/\sigma_r)^{1/2} \quad , \quad (3)$$

$$R = b - 10 \lg(f\mu_r/\sigma_r) \quad , \quad (4)$$

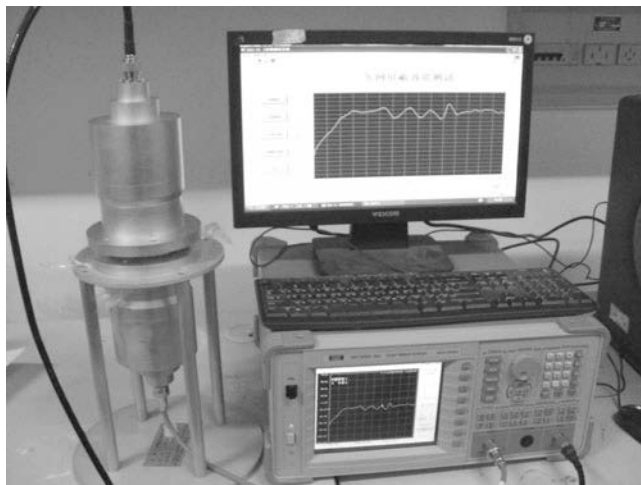


FIG. 8. DR-S01 tester for electromagnetic shielding effectiveness of planar materials.

TABLE I. Pore parameters of the cellular titanium foam.

Sample number	Mean pore-diameter (mm)	Sample thickness (cm)	Porosity (%)	Specific surface area $S_v$ ( $\text{cm}^2/\text{cm}^3$ )
1	~0.8	~1.0	~86	~400
2	~2.5	~1.2	~89	~450

$$B = 20 \lg(1 - e^{-2t/\delta}) \quad , \quad (5)$$

where both  $a$  and  $b$  are constants;  $f$  is the electromagnetic wave frequency (Hz);  $t$  is the shielding material thickness (mm);  $\sigma_r$  is the relative electrical conductivity;  $\mu_r$  is for the relative magnetic permeability;  $\delta$  is the skin depth, and:

$$\delta = (f\pi\sigma\mu)^{-1/2} \quad . \quad (6)$$

Equations (3) and (4) show the shielding effect of the material will be derived mainly from the reflection loss of electromagnetic waves at low frequencies, and mainly depend on the absorption loss within the material at high frequencies.

Figure 9 shows the electromagnetic shielding effectiveness for the cellular samples 1 and 2. It reveals that the shielding effectiveness of the sample gradually decreased from about 100 dB to about 25 dB with the increase of the frequency of electromagnetic waves in the range of 0–1000 MHz. After more than 1000 MHz, the shielding effectiveness of the sample showed a wavy platform, of which the center value is approximately 30–40 dB. In the entirely tested frequency range, the shielding effectiveness of sample 2 is slightly better than that of sample 1 below 1600 MHz, and is about the same at above 1600 MHz (the former may be only a little better than the latter).

The tested curves reveal that both samples showed a relatively high shielding effectiveness at relatively low frequencies in the testing range, which could not be high at relatively high frequencies. This is also in fact in agreement with that the mechanism of reflection loss would be dominant at low frequencies and that of absorption loss at high frequencies for the present titanium foam. In general, the content of metal solid in the high porosity foam is

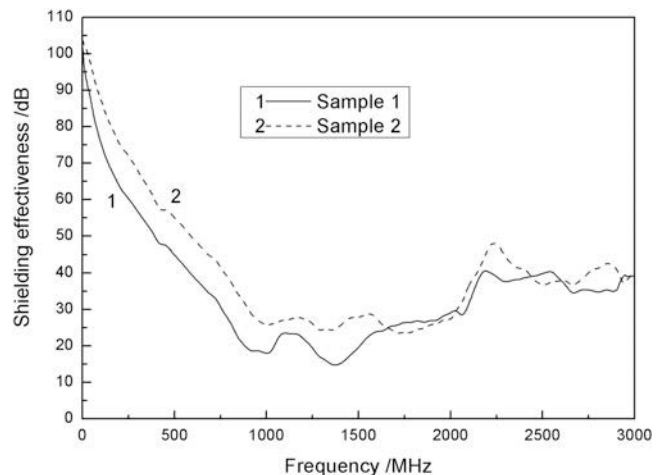


FIG. 9. Curves of relationship between electromagnetic shielding effectiveness and frequency for the cellular porous titanium foams.

relatively low, and the function that the loss mechanism can bring into play will be limited after all.

When the porosity is approximately equivalent and the pore size is not the same, the higher shielding effectiveness will occur to the foam sample with the smaller pore-size.<sup>21</sup> This is because that the smaller pore-size with a roughly equivalent porosity will mean a greater number of pores, and the number of the electromagnetic wave reflection inside the foam will increase, so that the absorption loss will also increase. In fact, this increase of the reflection should be substantially resulted from the more interface between the cell-wall and the air inside the foam, indicating a larger specific surface area of the foam, and not directly from the smaller pore-size. Of course, the smaller pore-size and the greater number of pores might make a larger specific surface area, which would be, however, also determined by another important factor, the porosity of the foam.

Reference 29 provides the calculation relation of specific surface area  $S_v$  for metal foams:

$$S_v \approx \frac{K_S}{d} \left[ (1 - \theta)^{\frac{1}{2}} - (1 - \theta) \right] \cdot (1 - \theta)^n \quad , \quad (7)$$

where  $S_v$  ( $\text{cm}^2/\text{cm}^3$ ) is the specific surface area of the metal foam;  $d$  (mm) and  $\theta$  (%) are the average pore-diameter and the porosity of the foam, respectively;  $K_S$  is a material constant that is determined by the material species and the preparation parameters for the porous body, and also what characterizes the material species of pore struts or walls and the structural and defective state;  $n$  is a geometric factor to characterize the pore structure of the foam, and it is affected by the specific structure mode of the material, so is finally also a constant that rests with the material species and the specific preparation process.

To the present cellular titanium foam, the data<sup>29</sup> resulted from the aluminum foam with the similar pore structure may be used, namely we may take  $n = 0.40$  and  $K_S = 281.8$  in Eq. (7), and then we have:

$$S_v \approx \frac{281.8}{d} \left[ (1 - \theta)^{\frac{1}{2}} - (1 - \theta) \right] \cdot (1 - \theta)^{0.4} \quad . \quad (8)$$

The specific surface area is calculated for the titanium foam by using the above equation, and the obtained results are also given in Table I. It is thus clear that the relatively large pore-sized sample (No. 2) with relatively high porosity has a larger value of specific surface area, and it was tested to be higher than the relatively small pore-sized sample (No. 1) with a smaller value of specific surface area in the shielding effectiveness at below 1600 MHz. A larger surface on the material may provide more sites to reflect the electromagnetic wave, namely, it will be more conductive to reflecting the electromagnetic wave. This is consistent with that the shielding effect

will be mainly derived from the reflection loss at low frequencies [see Eqs. (4) and (5)]. Another study result also shows that the shielding effectiveness of the porous structure increases with increasing the pore density when the porosity keeps roughly identical.<sup>23</sup> This is in essence due to a higher pore density (i.e., smaller pore size) in this case bringing a higher surface area to result in more reflections of electromagnetic waves in the porous structure.

Maybe it should be accounted for: the exponential value would more greatly influence the calculated result by using Eq. (7), in which taking  $n = 0.40$  and  $K_S = 281.8$  was for calculating the specific surface area of samples 1 and 2 based on the structural feature of cellular metal foams.<sup>29</sup> Consequently, a small change of the porosity could bring a large one of the specific surface area for highly porous metal foams. Accordingly, sample 2 would have a slightly larger value of the specific surface area than sample 1, although the porosity just increases from 86% for sample 1 to 89% for sample 2 and the mean pore-diameter performs a considerable increment from 0.8 mm for sample 1 to 2.5 mm for sample 2. Certainly, the relation will be another one different from Eq. (8) for the specific surface area of reticular metal foams, and this is closely related to their structural feature.

However, the absorption loss will play a more important role when the frequency of the electromagnetic field gets higher, and the contribution of reflection loss will decrease. The metal solid content is relatively higher for sample 1 with lower porosity, inside which there are thus more metal solid that will more powerfully interact with the electromagnetic field, so as to reinforce the absorption loss. In addition, the higher content of metal solid in the sample with lower porosity will lead to a larger conductivity, so a more absorption loss can also be directly inferred according to Eq. (3) for sample 1. The different loss mechanisms may jointly work at the same time, but will do severally to various extents when the specific condition changes. For sample 1 with more metal solid and sample 2 with larger surface area, the combined action both of the absorption and reflection loss mechanisms eventually induced a result that the shielding effectiveness would tend to being roughly equivalent in the case of higher frequencies.

Through the present data and the above analysis, we could conclude some general understandings in this work for the electromagnetic shielding performance of metal foams: for a certain type of structure of the metal foam used for a certain band of electromagnetic waves, the appropriate pore-size should be determined at first. In addition to this, the appropriate porosity would be then selected to achieve the maximum specific surface area for the low frequency shielding. For the higher frequency waves, the sufficient content of metallic solid need be also comprehensively considered, with the specific surface area as large as possible. That is to say, both the porosity

as low as possible and the specific surface area as large as possible need be endeavored to get for the foam used in the range of higher frequency: a lower porosity is to make a higher absorption loss, and a larger surface area is to make a higher reflection loss. Of these two kinds of losses, only the maximum summation can achieve the best result. However, reducing the porosity and increasing the specific surface area of the foam may be contradictory. Therefore, the relevant parameters need be determined according to the specific structure of the foam on the basis of Eq. (7), so as to find out the optimal matching between the porosity and the specific surface area for the different wave bands.

## V. CONCLUSIONS

(1) This work presents a sort of cellular titanium foam with spherically millimeter-scaled pores, which is a novel class of porous titanium material with high porosity of 86–90%. This titanium foam, belonging to a typical elastic-brittle porous material, presented a compressive curve that showed three regimes covering the initial elasticity, the zigzag compressive plateau, and the final “densification”. Such “densification” indicated a process that the broken pieces accumulated gradually. The compressive fracture occurred to be continually pushed forward by the pore collapse in the way of layer by layer in the direction perpendicular to loading. The pore layers located at the applied loading place and those weak positions would be both preferentially ruined.

(2) The present cellular titanium foam exhibited an evident effectiveness of electromagnetic shielding, which decreased with the increase of the electromagnetic wave frequency in the range of 0.3–1000 MHz, and the corresponding curve presented a relatively long platform when the frequency is between about 1000 and 3000 MHz. The shielding mechanism of such samples could be mainly by the reflection loss in the low frequency region and by the absorption loss in the relatively high frequency range. Because the content of metallic solid in the highly porous foam would be relatively low the loss mechanism could play just a limited role. Therefore, the above-mentioned platform area would appear in the low value zone of the whole shielding effectiveness curve.

## ACKNOWLEDGMENTS

The financial support of the Testing Foundation (C15) of Beijing Normal University and the experimental assistance of Mr. H.B. Qing in sample preparation and SEM observation are both greatly appreciated.

## REFERENCES

1. M.F. Ashby, A. Evans, N.A. Fleck, L.J. Gibson, J.W. Hutchinson, and H.N.G. Wadley: *Metal Foams: A Design Guide* (Elsevier Science, Boston, 2000).

2. J. Banhart: Manufacture, characterisation and application of cellular metals and metal foams. *Prog. Mater. Sci.* **46**, 559–632 (2001).
3. P.S. Liu and K.M. Liang: Functional materials of porous metals made by P/M, electroplating and some other techniques. *J. Mater. Sci.* **36**, 5059–5072 (2001).
4. F. Barari, E.M.E. Luna, R. Goodall, and R. Woolley: Metal foam regenerators, heat transfer and storage in porous metals. *J. Mater. Res.* **28**(17), 2474–2482 (2013).
5. P.S. Liu and G.F. Chen: *Porous Materials* (Elsevier Science, Boston, 2014).
6. C.E. Wen, J.Y. Xiong, Y.C. Li, and P.D. Hodgson: Porous shape memory alloy scaffolds for biomedical applications: A review. *Phys. Scr.* **T139**, 014070 (2010).
7. A. Bansiddhi and D.C. Dunand: Shape-memory NiTi-Nb foams. *J. Mater. Res.* **24**(6), 2107–2117 (2009).
8. D.P. Mondal, J.D. Majumder, N. Jha, A. Badkul, S. Das, A. Patel, and G. Gupta: Titanium-cenosphere syntactic foam made through powder metallurgy route. *Mater. Des.* **34**, 82–89 (2012).
9. X. Rao, C.L. Chu, and Y.Y. Zheng: Phase composition, microstructure, and mechanical properties of porous Ti-Nb-Zr alloys prepared by a two-step foaming powder metallurgy method. *J. Mech. Behav. Biomed. Mater.* **34**, 27–36 (2014).
10. L.P. Lefebvre and E. Baril: Properties of titanium foams for biomedical applications. *Adv. Eng. Mater.* **15**, 159–165 (2013).
11. C.E. Wen, Y. Yamada, K. Shimojima, Y. Chino, H. Hosokawa, and M. Mabuchi: Novel titanium foam for bone tissue engineering. *J. Mater. Res.* **17**(10), 2633–2639 (2002).
12. M. Takemoto, S. Fujibayashi, M. Neo, J. Suzuki, T. Kokubo, and T. Nakamura: Mechanical properties and osteoconductivity of porous bioactive titanium. *Biomaterials* **26**(30), 6014–6023 (2005).
13. G.I. Nakas, A.F. Dericioglu, and S. Bor: Monotonic and cyclic compressive behavior of superelastic TiNi foams processed by sintering using magnesium space holder technique. *Mater. Sci. Eng., A* **582**, 140–146 (2013).
14. T. Imwinkelried: Mechanical properties of open-pore titanium foam. *J. Biomed. Mater. Res. A* **81**, 964–970 (2007).
15. J. Rivard, V. Brailovski, S. Dubinskiy, and S. Prokoshkin: Fabrication, morphology and mechanical properties of Ti and metastable Ti-based alloy foams for biomedical applications. *Mater. Sci. Eng., C* **45**, 421–433 (2014).
16. M.S. Aly: Behavior of closed cell aluminium foams upon compressive testing at elevated temperatures: Experimental results. *Mater. Lett.* **61**(14–15), 3138–3141 (2007).
17. N. Resnina, S. Belyaev, A. Voronkov, A. Krivosheev, and I. Ostapov: Peculiarities of mechanical behaviour of porous TiNi alloy, prepared by self-propagating high-temperature synthesis. *Mater. Sci. Eng., A* **527**(23), 6364–6367 (2010).
18. L.P. Lefebvre, E. Baril, and L. de Camaret: The effect of oxygen, nitrogen and carbon on the microstructure and compression properties of titanium foams. *J. Mater. Res.* **28**(17), 2453–2460 (2013).
19. H. Bafti and A. Habibolahzadeh: Compressive properties of aluminum foam produced by powder-Carbamide spacer route. *Mater. Des.* **52**, 404–411 (2013).
20. S. Frackowiak, J. Ludwiczak, K. Leluk, K. Orzechowski, and M. Kozłowski: Foamed poly(lactic acid) composites with carbonaceous fillers for electromagnetic shielding. *Mater. Des.* **65**, 749–756 (2015).
21. Y. Feng, H.W. Zheng, Z.G. Zhu, and N. Tao: Electromagnetic shielding effectiveness of closed-cell aluminum alloy foams. *Chin. J. Nonferrous Met.* **14**(1), 33–36 (2004).
22. Z.B. Xu and H. Hao: Electromagnetic interference shielding effectiveness of aluminum foams with different porosity. *J. Alloys Compd.* **617**, 207–213 (2014).

23. K.J. Ji, H.H. Zhao, Z.G. Huang, and Z.D. Dai: Performance of open-cell foam of Cu-Ni alloy integrated with graphene as a shield against electromagnetic interference. *Mater. Lett.* **122**, 244–247 (2014).
24. L.B. Wang, K.Y. See, Y. Ling, and W.J. Koh: Study of metal foams for architectural electromagnetic shielding. *J. Mater. Civ. Eng.* **24**(4), 488–493 (2012).
25. J. Iniguez, V. Raposo, A.G. Flores, M. Zazo, and P. Hernandez-Gomez: Advantages of the use of metal foam for electromagnetic shielding. *Key Eng. Mater.* **543**, 125–128 (2013).
26. L.J. Gibson and M.F. Ashby: *Cellular Solids: Structure and Properties* (Cambridge University Press, Cambridge, 1999).
27. P. Xiang, H.F. Cheng, L.E. Mo, and L.L. Cao: Electromagnetic shielding effectiveness of open-cell aluminum foam. *Met. Funct. Mater.* **15**(1), 12–15 (2008).
28. X.L. Huang, G.H. Wu, Q. Zhang, L.T. Jiang, and X. Chen: Electromagnetic shielding properties of open-pore Fe-Ni foams. *Rare Met. Mater. Eng.* **39**(4), 731–734 (2010).
29. P.S. Liu: A new method for calculating the specific surface area of porous metal foams. *Philos. Mag. Lett.* **90**(6), 447–453 (2010).